

Winning the Global Race for Solar Silicon

David Lynch

Enhanced for the Web

This article appears on the JOM web site (www.tms.org/jom.html) in html format and includes links to additional on-line resources.

While there are numerous contestants in the race to produce low-cost solar silicon, the chemistries involved can be grouped into three categories: new Siemens-like processes, new approaches to reduction of silica, and upgrades of metallurgical-grade silicon. This review is focused on the thermo-chemistries being employed in the last two categories, with emphasis on removal of boron and phosphorous, as these elements are the two most difficult to remove from silicon by unidirectional solidification.

INTRODUCTION

Historically, the photovoltaic (PV) industry relied on off-spec electronic-grade silicon (e-Si) as its primary raw material. That silicon, produced through the Siemens Process, is both costly and far purer (nine 9s) than that necessary for PVs.¹ With growing demand, it was only a matter of time before there was a shortage of silicon for PVs. The first shortage occurred in 1996/97 with the price of silicon rising to \$75 per kg on the spot market, three times the production cost at that time.¹ That shortage quickly disappeared, only to reappear in 2003 with the spot market price rising to \$450 per kg in 2008.² Since the recent economic downturn, the spot market price fell to \$75 per kg by the end of May.³ By the time this manuscript is published the price will likely be \$50 per kg or lower.²

While conditions that brought about the latest shortage have eased, the insatiable desire for energy and the political

How would you...

...describe the overall significance of this paper?

This paper provides a mix of thermo-chemistry, thermodynamics, and economics while reviewing research and developments aimed at capitalizing on the growth of the photovoltaic industry. Much of the manuscript is focused on the thermo-chemistry of boron and phosphorus, and the behavior of those elements during reduction of silica and refining of silicon. These are the two most difficult elements to remove from silicon and the two elements that dictate success or failure in producing low-cost solar silicon by metallurgical means.

...describe this work to a materials science and engineering professional with no experience in your technical specialty?

This article uses chemical thermodynamics and physical chemistry to evaluate literature involving tramp elements in the silicon submerged arc furnace, and during the refining of silicon. With respect to refining processes, much of the focus is on boron and phosphorus, and the thermo-chemical behavior of those elements during slagging, silicide formation, recrystallization, and volatilization by e-beam melting, plasma heating, and chemical reaction.

...describe this work to a layperson?

This article takes a broad view of the thermo-chemistry being employed to develop a process for producing low-cost solar silicon. Historically, the photovoltaic industry relied on off-spec electronic-grade silicon as its primary raw material. That silicon is costly and far purer than necessary for solar cells. Technical advancements in other areas along the value chain have left the raw material cost of silicon as the single largest contributor to the cost of producing solar cells.

will of many countries to curb CO₂ emissions assures that demand for PVs will continue to grow. There are only a few PV materials with known reserves that can contribute at the tera-Watt-year level needed to meet the estimated shortfall in electrical energy.⁴ Silicon dominates 90% of the PV market today. While that percentage is expected to decline to 33% by 2030,⁵ historic annual growth rates of more than 30% for new installed PV capacity, as shown in Figure 1, suggests a growing future for silicon and other PV materials. The phenomenal growth rate has been due largely to the willingness of a few countries to provide subsidies. Undoubtedly, the annual growth rate for 2009 will be lower, reflecting the downturn in the economy and reduction in subsidies. However, the cost of silicon is expected to again approach the production cost for silicon produced in the Siemens Process, now estimated to be \$30–40 per kg.

Silicon-based PVs can play a far greater role in meeting the world's need for electrical energy, given its plentiful supply, but only if cost reductions along the entire production chain can be achieved. Silicon amounts to more than 25% of the cost of producing PV panels made from polysilicon, and as much as 40% for single-crystal silicon systems. The target cost in the race to produce 6-nines pure s-Si is \$15 per kg.

Production and refining of silicon for manufacture of PVs begins with the silicon submerged arc furnace and ends with unidirectional solidification (UDS). The latter is essential for producing an ingot for wire sawing, but it can also be the last step in refining. What happens to boron and phosphorous in the arc furnace up to UDS in producing s-Si by metallurgical means is the focus of this manuscript.

IMPURITIES IN THE SILICON SUBMERGED ARC FURNACE

An understanding of the presence of impurities in silicon, particularly boron and phosphorous, begins with examination of the thermo-chemistry of the arc furnace for which a partial cross section is presented in Figure 2. The kettle, containing the silicon and charge, is rotated once every 20 to 30 days, and results in cavities forming around each electrode. The cavities play a critical role in a physico-chemical process in the production of silicon. Cavity temperatures vary from 2,200 K at the top to 2,400 K at the bottom of the electrode.

At these temperatures kinetic processes will be fast, and thermodynamic equilibrium becomes the dominant factor as to what takes place in the furnace. The Si/SiO₂ equilibrium line in the Ellingham diagram in Figure 3 delineates oxides above the line that are reduced in the furnace, and those below the line that are partially reduced through dissolution of the metal atom in molten silicon and formation of SiO₂ or SiO(g). The high temperatures and the reducing conditions in the arc furnace led Myrhaug and Tveit⁷ to develop a boiling point model for 30 impurity elements, which they tested by conducting mass balances.

Elements, such as boron, with a normal boiling point temperature above the highest temperature in the submerged arc furnace were expected to leave the furnace in the product, whereas elements with boiling point temperatures below that of the top bed temperature in the furnace, like phosphorous, were expected to leave the furnace in the flue gas. Elements with temperatures in between the two limits were expected to distribute between the silicon, flue gas, and silica fume. The results of the mass balances presented in Figure 4 reveal that industrial practice is in agreement with the model, with the most serious disagreement involving phosphorous. The model predicts that all phosphorous should be volatilized, whereas the mass balance reveals that 75% of the phosphorous left the furnace in the silicon.

The presence of both boron and phosphorous in m-Si poses a serious problem for companies seeking to produce s-Si by metallurgical processes. While other impurity elements readily respond to purification by UDS, phosphorous responds weakly and boron not at all.

Phosphorus in the Arc Furnace

Quartz, in ball size chunks of 5–8 cm in diameter, charged to the arc furnace contains apatite (Ca₃(PO₄)₂) and iron oxides, both sealed within the rock.^{7,8} As

quartz is heated, iron oxides fuse with the silica, forming droplets of slag that dissolves apatite. Only after the fused and viscous silica enters the cavity in the furnace and contacts molten silicon are the small droplets of slag exposed to reducing conditions, where the iron oxide in the slag is reduced and the resulting elemental iron reacts with the phosphorous in the slag, forming an Fe-P alloy.⁹

Phosphorous is far less volatile in molten iron than silicon. Volatility of phosphorous is linked directly to the activity coefficient of phosphorous in the alloy, f_p , shown in Figure 5. The 1 wt.% standard state values for f_p are with respect to the Si-P alloy, where f_p has a value of 1. Negative values for $\log f_p$ reflect less volatility for phosphorous than that in molten silicon, and positive values greater volatility. Maximum volatility occurs at a composition corresponding closely with FeSi₂, suggesting preferred bonding between silicon and iron supplants bonding between iron and phosphorous. Only when the iron content in the Fe-Si alloy exceeds 65 wt.% is the volatility of phosphorous in solution below that of phosphorous in molten silicon.¹⁰

The volatility of P₂(g) in equilibrium with an Si-Fe alloy at 1,800 K is presented in Figure 6, having been computed using the data in Figure 5.⁹ Point "A" in the diagram corresponds to

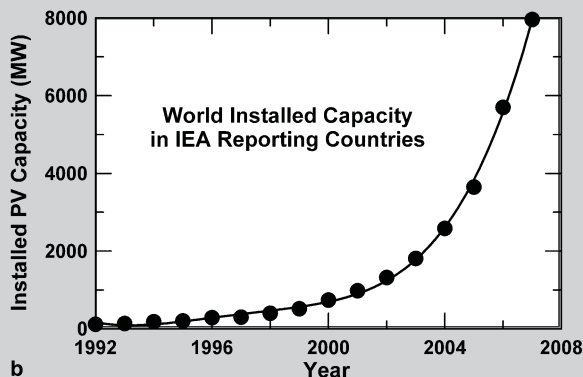
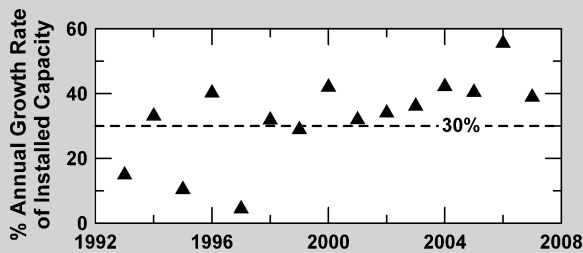


Figure 1. Growth in PVs as reported by the International Energy Association (IEA).

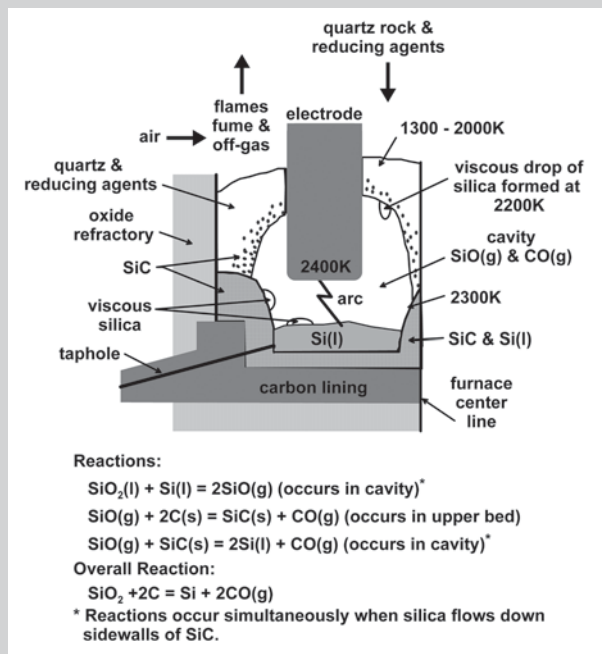


Figure 2. Partial cross section of silicon submerged arc furnace and chemical reactions, after Ref. 6.

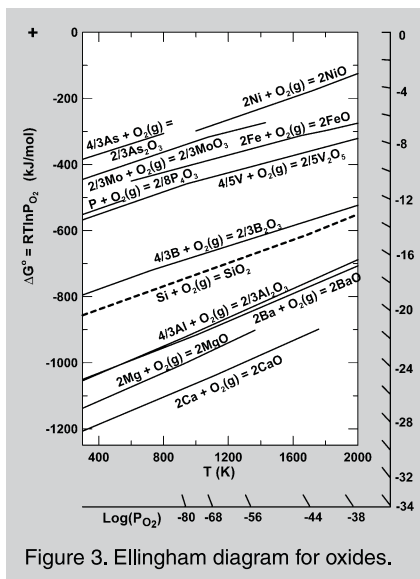


Figure 3. Ellingham diagram for oxides.

molten iron with 1.5 wt.% phosphorous with the vapor pressure of P_2 equal to approximately 10^{-9} bar. Incremental addition of silicon to molten iron leads to a significant increase in $P_2(g)$ with only a modest reduction in the concentration of phosphorous in the alloy along the path from point A to B. Point B corresponds to 50 wt.% iron. Further addition of silicon to the alloy leads to significant decline in both $P_2(g)$ and concentration of phosphorous in the alloy, the process following conditions from point B to C. Points A and C have nearly the same value of $P_2(g)$, but the concentration of phosphorous in iron versus that in silicon is nearly three orders of magnitude greater, reflecting the stabilizing effect of iron on phosphorous at high temperatures.

If silicon is added incrementally to the Fe-P droplets once exposed to the furnace environment, phosphorous can be volatilized. Unfortunately, lumps of viscous silica, containing droplets of the alloy, fall into the pool of molten silicon or flow down the walls of the cavity into the pool, where reaction of SiO_2 with silicon produces $SiO(g)$. That reaction exposes droplets of slag to reducing conditions in the cavity that leads to the formation of the Fe-P alloy, but in the presence of excess silicon that quickly dilutes the alloy, a condition characterized by the path A-C in Figure 6. Since reaction between SiO_2 and silicon is key to producing silicon, as indicated by the reactions in Figure 2, nearly all phosphorous entering the arc furnace in quartz finds its way to the silicon.

Producers of s-Si seek quartz with phosphorous content below 5 ppmw, whereas producers of m-Si process quartz with less than 50 ppmw phosphorous.^{7,11} Forty-five percent of the phosphorous enters the arc furnace in the quartz, 45% in the reducing agents, and 10% in the electrodes.⁷ The mass balance for phosphorous in Figure 4 reveals that 25% of the phosphorous leaves the furnace with silica fume, and assuming all the phosphorous in the quartz rock leaves the furnace in the silicon, it is estimated that processing phosphorous-free quartz in the arc furnace will lead to a 60% reduction of phosphorous in the product. Since a typical value of phosphorous in m-Si is 30 ppmw, processing phosphorous-free quartz with conventional reducing agents and electrodes would yield silicon with a phosphorous content of 12 ppmw, not the 1 ppmw or less required for s-Si.

The likely source of the 25% of the phosphorous leaving the arc furnace in silica fume is reducing agents. Pre-processing of electrodes at 1,523 K ensures that phosphorous in that source is chemically stabilized, most likely with iron impurity. Fume forms just above the top of the bed where $SiO(g)$ mixes with air and phosphorous condensed on the silica fume (most likely as an oxide), suggesting that much of the phosphorous in reducing agents is not physically trapped as in the quartz rock. For those seeking to produce s-Si, a look at the chemistry of phosphorous in reducing agents could pay dividends.

Boron in the Arc Furnace

More than 95% of the boron entering the arc furnace leaves in the silicon.⁷ The high boiling point temperature of boron leaves one option for significantly reducing its concentration in the product: processing materials free of boron. Since 37% of boron enters with the quartz and 61% in the reducing materials,⁷ the reduction of boron content in silicon is directly linked to the impurity level in those two sources.

ACID TREATMENT

Elkem's 1985 patent for purification of m-Si by the Silgrain Process discloses that some acid treatments of solidified silicon yielded 90% removal of phosphorous.¹² It is essential to examine what takes place in the Silgrain Process before exploring how phosphorous may have been removed in the process.

Purification of m-Si by the Silgrain Process begins by maintaining a calcium-to-iron molar ratio in molten silicon greater than 14, so that $CaSi_2$ precipitates around primary grains of silicon.¹³ Further removal of impurities involves precipitation of other silicides. Treatment of the lumps of solidified material with 5% HCl solution leads to chlorination of $CaSi_2$ and formation of the "yellow phase" that swells, cracking open the lumps and exposing all the $CaSi_2$ to further reaction with acid. The primary grains of silicon do not react with the HCl solution. Warm water is used to remove the water-soluble yel-

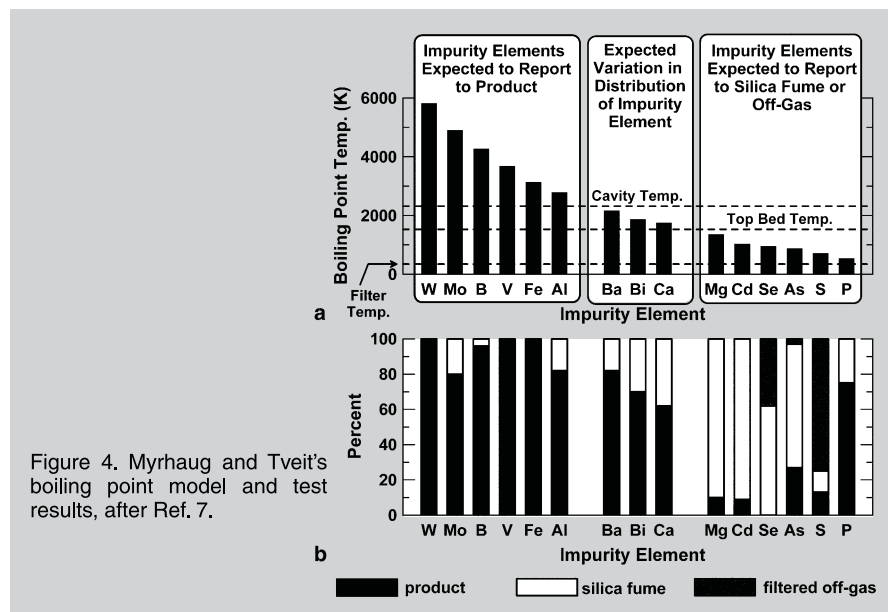


Figure 4. Myrhaug and Tveit's boiling point model and test results, after Ref. 7.

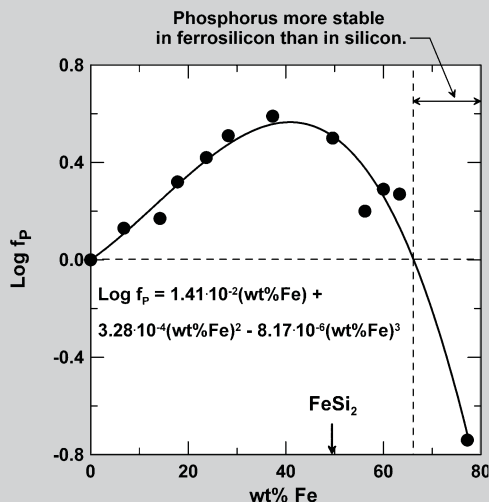


Figure 5. Activity coefficient of P in Si-Fe molten alloys at 1,723 K, data from Ref. 10.

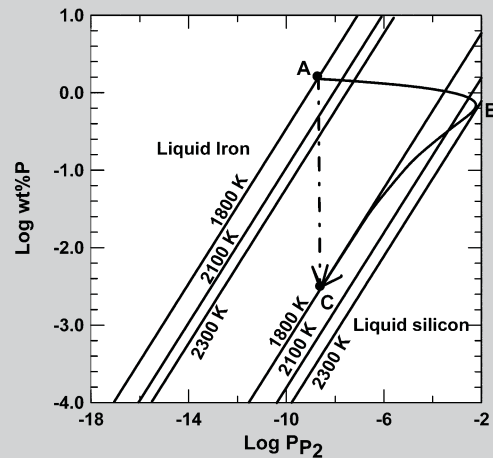


Figure 6. Volatility of P; route A-B-C gradual addition of Si to Fe-P alloy, and route A-C alloy quenched in pool of molten Si.

low phase and its impurity elements, followed by treatment of the grains of silicon with weak HF solution to remove a thin layer of SiO₂ surrounding the silicon, a layer also containing impurity elements. Again, the impurities are washed away.

Removal of phosphorous from silicon through the Silgrain Process must involve formation of phosphides. The Ellingham diagram for phosphides in Figure 7 reveals that SiP is one of the least stable phosphides, and that Fe, Al, Mn, Co, Mg, and Ca would preferentially form phosphides first with respect to silicon, except for the fact that those impurity elements are present in the silicon at low concentrations. With silicon present in excess, it is necessary to examine the ability of phosphorous to disrupt the bonding between silicon and the impurity elements.¹⁴ That is accomplished by examining the ability of P₂(g) to form phosphides from silicides, using the Ellingham diagram in Figure 8. While the diagram in Figure 7 indicates that calcium forms the most stable phosphide, the thermodynamic calculations presented in Figure 8 suggest that magnesium dissolved in silicon appears to have the greatest ability to form a phosphide. The actual situation is complex; one must take into account that some elements don't form mono-silicides and thus aren't included in Figure 8, and all elements appear to form binary, ternary, and more complex silicides for which there are no thermodynamic data. Additional issues involve the concentration of impurity elements and their activity in silicon. While Mg

appears to be more suited for forming a phosphide, there is far greater concentration of Al, Ca, and Fe in m-Si than Mg. Phosphide formation is not strictly a thermodynamic issue, but involves kinetics and transport issues as well.

REFINING

The "Holy Grail" for those seeking to refine silicon for PVs is a single economic process whereby both boron and phosphorous are removed to acceptable concentrations. Thus, research into refining silicon has focused on those elements.

Boron

The earliest refining process for boron involved gas injection and volatilization of boron-containing compounds. More recently the focus has been on slagging.

Volatilization of boron from molten silicon was linked to H₂-H₂O vapor by Theuerer,¹⁵ who reported that during zone refining of silicon, inclusion of water vapor with the protective H₂ atmosphere significantly increases the resistivity of silicon—a result attributed to volatilization of boron-containing species.

Theuerer's results no doubt inspired researchers to pursue this approach. An early report set the vapor pressures of BO, BO₂, and B₂O₃ at values of 74, 0.15, and 0.056 Pa, respectively, for treatment of molten silicon at 2,273 K.¹⁶ Using available data for the activity of boron in molten silicon,¹⁴ assuming the initial boron content in the silicon to be 15 ppmw, and using the maximum p_{O₂} associated with the Si-SiO₂ equilibrium, the vapor

pressures of the oxides are computed to be no larger than 0.54, 1.2·10⁻³, and 7.7·10⁻⁴ Pa, respectively. (Typical boron content in metallurgical silicon today ranges from 15 to 20 ppmw.) Further thermodynamic analysis indicates that the prominent boron species volatilized with an H₂-H₂O gas injection is likely HBO, and not the oxides. The volatility of HBO has been computed, and results plotted in Figure 9 for the conditions used to compute the latest partial pressures for the oxides. The diagram includes the conditions beyond which SiO(g) exists at a pressure of 1 bar, the practical limit for sparging with H₂-H₂O. Generation of SiO(g) can't be stopped, as it decomposes to SiO₂ and silicon upon contacting a cooler surface. The maximum vapor pressure of HBO at 1 bar total pressure is limited to about 5 Pa and will decline significantly as boron is volatilized. A large volume of gas will be required, and substantial loss of silicon by SiO volatilization will occur.

Boron removal by distribution with oxide slags is largely based on the research of Suzuki et al.,¹⁷ and Fujiwara and co-workers.¹⁸ A summary of their experimental results is presented in Figure 10 where the distribution of boron between slag and silicon is plotted versus slag composition. The distinct feature in the diagram is the maximum occurring in all cases near the orthosilicate, as represented where the ratio of the mole fractions of CaO to SiO₂ is equal to 2. The orthosilicate occurs at smaller values of the ratio in slags containing BaO and MgO. The refining capability for boron (i.e., formation of BO₃³⁻ ions in slag) is

dependent on the activity of SiO_2 and the concentration of oxygen anions (O^{2-}) in the slag, as indicated by the chemical reaction in the figure. Unfortunately, a rise in the value of one leads to a decline in the other, producing a maximum distribution of boron between slag and silicon at the orthosilicate.¹⁹

Phosphorus

Efforts to remove phosphorous from silicon have involved volatilization combined with vacuum treatment, and slagging. Volatilization of a solute is usually based on the vapor pressure of the solute being greater than that of the solvent. The opposite is the case for elimination of phosphorous from silicon, but the mass of phosphorous is small and thus the loss of silicon is acceptable. At 1,973 K the equilibrium molar ratio of phosphorous to silicon, in the vapor phase, ranges from $2 \cdot 10^{-4}$ to $7 \cdot 10^{-6}$ as the concentration of phosphorous is reduced from 30 ppmw to 1 ppmw, while it is computed that 290 moles of silicon are lost per mole of phosphorous volatilized. That loss, while appearing to be significant, amounts to less than 1% of the silicon refined.

Experimental results in Table I reveal that volatilization at elevated temperatures is effective for removing many elements. Pires et al.²⁰ used e-beam vacuum heating to fuse silicon buttons 25 mm thick and 90 mm in diameter over a period of 20 minutes at e-beam power levels of 15 to 17 kW at pressures of 10^{-4} to 10^{-2} Pa. A comparison of results in Table I with the boiling point temperatures in Figure 4 suggests, as a result of significant reduction of aluminum content by e-beam melting, that surface temperature of the silicon buttons was approaching that of the boiling point of aluminum. Unfortunately, as might be expected from boiling point temperatures, boron content is not reduced to the desired concentration of 1 ppmw for solar silicon, nor can it as its boiling temperature is greater than that of silicon. Thus a separate refining step for boron is required.

Research into distribution of phosphorous between silicon and slag has largely focused on the impact of CaO in slag reacting with phosphorous in silicon, forming Ca_3P_2 that dissolves in the slag. The ionic form of the reaction

is included in Figure 11b. Much of the attention on CaO is based on the thermodynamic stability of Ca_3P_2 observed in Figure 7.

Tabuchi and Sano²¹ measured the solubility of phosphorous in the CaO-CaF₂ melts by equilibrating phosphorous vapor with the melt at various partial pressures of O_2 . They showed that equilibrium can be represented by the reaction in Figure 11 where the source of oxygen anions is CaO and the negative charge on the P^{3-} anion in slag is neutralized by the Ca^{2+} cations. The data in Figure 11 indicate that reducing the partial pressure of O_2 increases the solubility of phosphorous in slag; the chemical reaction in the diagram suggests that selection of a slag where it is possible to increase the O^{2-} ion content (i.e., increasing the slag basicity) will further improve solubility of phosphorous in slag.

Those conclusions, based on experimental results obtained with a system absent elemental silicon, are only partially correct. Decreasing p_{O_2} and increasing the basicity of slag by the addition of CaO to slag in the presence of molten silicon leads to increased concentration of calcium in the silicon, and in turn increased concentration of phosphorous in that phase. The presence of additional calcium can, through ternary interaction, draw phosphorous from slag back into molten silicon. While CaO is a very

stable oxide, as the data in Figure 3 supports, preferred bonding between calcium and silicon, and formation of SiO_2 (or $\text{SiO}(\text{g})$) leads to the decomposition of the oxide and increased concentration of calcium in silicon. The extent of preferred bonding between calcium and silicon can be quantitatively evaluated by comparing Henrian activity coefficients (γ_i°) for solutes in molten silicon.^{14,22-26} That comparison is available in Figure 12, where calcium is, by virtue of its position at the bottom of the diagram, the most stable solute. Thermodynamic data for the formation of CaO and SiO_2 and the value of γ_{Ca}° in Figure 12 at 1,773 K were used to compute the solubility of calcium in molten silicon, and the activity of SiO_2 in slag at CaO saturation and for values of p_{O_2} in Figure 11. Those results included in the upper graph in the figure indicate that at the lowest value of p_{O_2} the mole fraction of calcium in the silicon (X_{Ca}) is in excess of 0.1. Also it is clear that much of the solubility data in the lower graph is at values of p_{O_2} above the saturation level for SiO_2 , and not applicable for refining of silicon.

The ternary impact of deoxidizing agents on the solubility of oxygen dissolved in molten iron produces a minimum solubility of oxygen, followed by increasing concentration of oxygen with increasing content of the deoxidizing agent.²⁷ Increasing concentration of

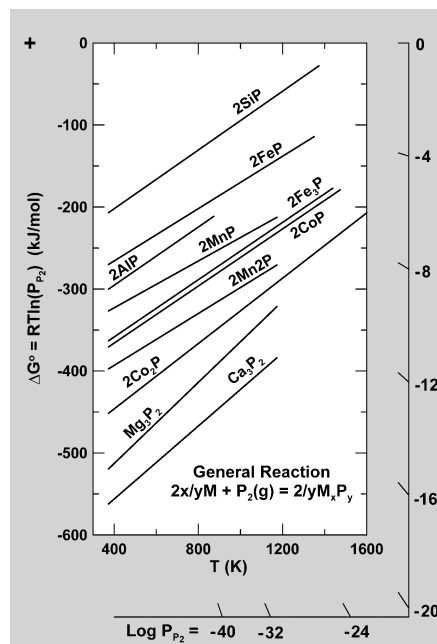


Figure 7. Ellingham diagram for phosphides.

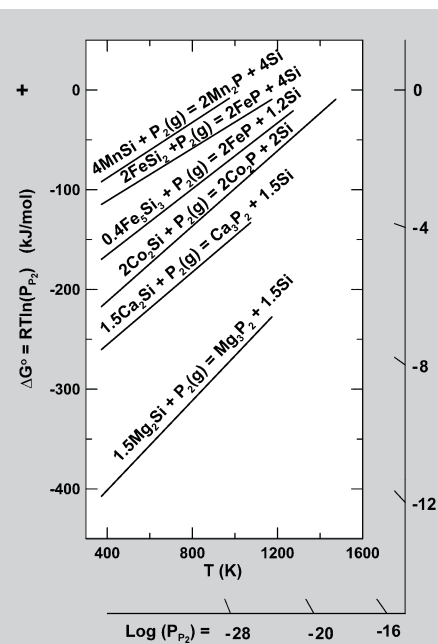


Figure 8. Ellingham diagram contrasting stability of phosphide versus silicide.

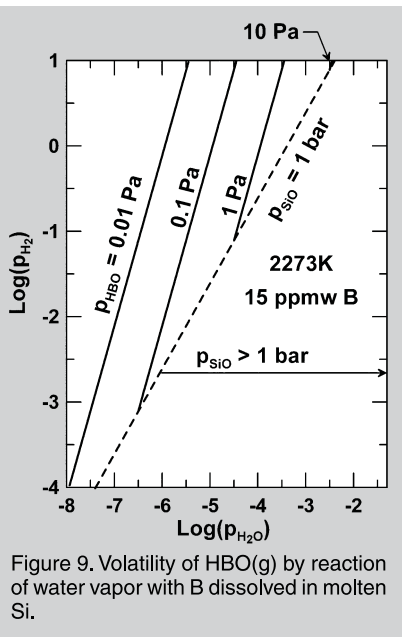


Figure 9. Volatility of HBO(g) by reaction of water vapor with B dissolved in molten Si.

calcium in molten silicon has the same impact on the solubility of phosphorous. However, when the ternary effect is viewed through the distribution of phosphorous between slag and silicon, a maximum is observed as shown in Figure 13. The final concentration of calcium in the silicon, provided in parentheses with each data point, show a marked increase with increasing CaO content in slag. The impact of the ternary effect leads to greater retention of phosphorous in molten silicon.

SOLIDIFICATION REFINING

Refining by UDS, an established procedure, moves impurity elements to one end of an ingot. The procedure is well documented in the literature,²⁹ and thus not considered further, except to note that it has no impact on removing boron from silicon, and can reduce phosphorous content to 35% of the initial concentration in the molten alloy for the first material solidified; at 80% solidification the content of phosphorous in the ingot is at approximately 85% of the initial concentration. The overall phosphorous content of the ingot (at 80% solidification) is approximately one-half the initial concentration. Thus m-Si with 30 ppmw phosphorous will produce an ingot with a concentration ranging from 10 to 26 ppmw phosphorous with a single UDS, but with an overall phosphorous content of 15 ppmw. Second and third UDS procedures produce ingots with overall phosphorous content of 7.5 and 3.8 ppmw, respectively. The variation in the

phosphorous content in the final ingot ranges from 2.6 to 6.4 ppmw. Cropping the top 20% of each fully solidified ingot produces a final yield of refined silicon of 50 percent with three UDS steps.

An alternative approach to UDS is recrystallization from an alloy.^{30,31} Silicon must be the primary phase solidified, and the only phase solidified. Aluminum is one element that does not form a mono-silicide, and thus has received considerable attention as a solvent for silicon recrystallization. It also has the advantage of having a melting temperature substantially lower than silicon, and forms a eutectic point at 850 K at 87.4 wt.% silicon. Use of aluminum as solvent allows for low temperature solidification over a wide composition range for the alloy.

Morita and co-workers examined the ability of using aluminum as solvent for recrystallization of silicon.³¹⁻³³ Some of their results for the measured segregation coefficients for impurities, k_i , are presented in Figure 14. The coefficient is the ratio of the mole fraction of the impurity in the silicon solidified versus the mole fraction of that element in the molten alloy. The smaller the value of k_i the greater is the extent of removal of that element from solid silicon. Unfortunately, recrystallization of silicon from an Si-Al alloy has the least impact on removal of boron and phosphorous.

CONCLUSIONS

How to Win the Race for Solar Silicon

Limiting factors that impact the potential of using a metallurgical route for producing s-Si were examined. If these factors are truly limiting, what are the options for producing s-Si?

Carbothermic Reduction of Silica

Myrhaug and Tveit's⁷ boiling point model and subsequent mass balances for production of ferrosilicon in a submerged arc furnace provide information as to the source of impurity elements and the extent to which they end up in the product. If s-Si is to be produced directly from quartz and reducing agents they must be substantially free of impurity element, with no more than a total impurity content of 1 ppmw per kg of silicon produced. If the intent is to pro-

Table I. Impact of E-Beam Refining²⁰

Element	Impurity Level in As-received Si (ppmw)	Impurity Level after E-beam Melting (ppmw)
Al	110.00	0.44
B	10.00	7.30
Ca	26.00	0.31
Fe	790.00	0.70
P	38.00	0.39
Total Impurity	1108	5.165
Si (%)	99.88	99.9995

duce low boron and phosphorous content silicon that is to be further refined by UDS, the limitation applies to those elements only.

FESIL is developing the Solsilc Process,³⁴ where high-purity quartz and reducing agents are being processed. Natural gas is cracked to produce a high-purity carbon black that is combined with quartz and SiC fines using a high-purity binder. No wood chips or coal, which are significant sources of impurities, are used in the reduction process. The higher cost of raw materials is offset by fewer refining steps.

Fine grain deposits of silica sand exist. Those sands with low impurity content can be autoclaved with an acid wash or other solvent to further cleanse them of impurities; for example $\text{Ca}_3(\text{PO}_4)_2$ is soluble in dilute acid and B_2O_3 is soluble in water and ethanol. The finer the sand the greater the surface area per unit vol-

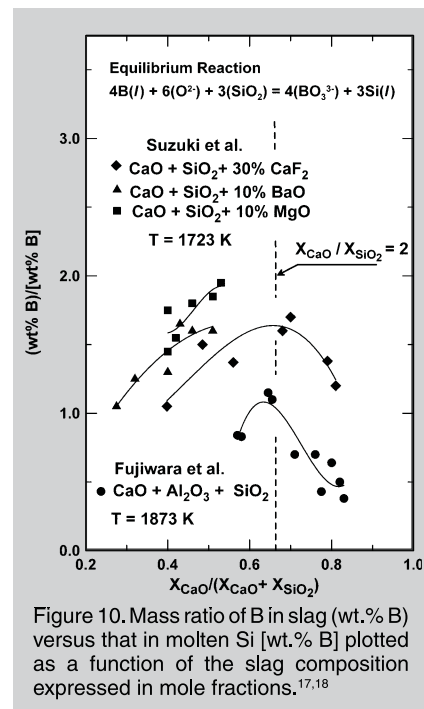


Figure 10. Mass ratio of B in slag (wt.% B) versus that in molten Si [wt.% B] plotted as a function of the slag composition expressed in mole fractions.^{17,18}

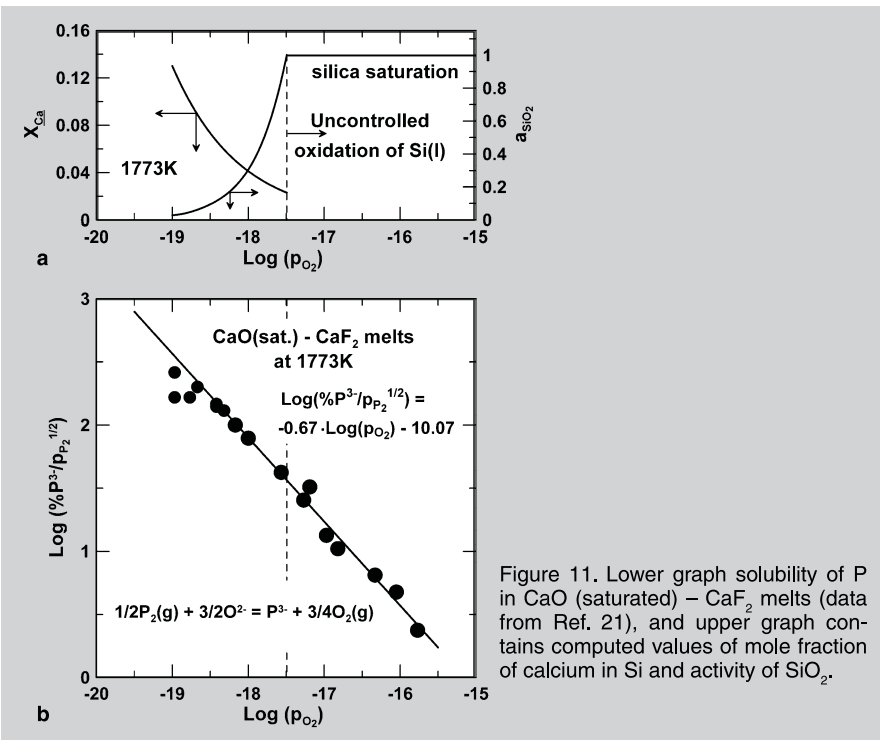


Figure 11. Lower graph solubility of P in CaO (saturated) – CaF₂ melts (data from Ref. 21), and upper graph contains computed values of mole fraction of calcium in Si and activity of SiO₂.

ume and the greater the probability that impurities can be removed by this process. The recovered silica can be mixed with high-purity reducing agents and consolidated by sintering or with a high-purity binder, and then processed in an arc furnace.

Acid Treatment

Removal of 90% of the phosphorous in m-Si by acid treatment, as reported in Elkem's patent,¹² can reduce the phosphorous content from 30 to 3 ppmw. Following the procedure described with respect to solidification refining, a single UDS will produce an ingot with phosphorous content varying between 1 and 2.6 ppmw, with 80% yield.

Volatilization

Volatilization techniques are limited by low vapor pressures of volatiles. The issue is made difficult by the initial low concentration of elements to be volatilized and their decreasing concentration during processing. Large volumes of gas are required and must be effectively distributed through the silicon. Long process times are required. A combination of different sparging gases with slag formation can speed the refining process.

The sparging gas is eliminated in e-beam heating, but the heating must be conducted under ultra-high vacuum that severely impacts the economics of volatilizing impurities. Heating is limited to

a thin layer no more than 1 to 3 cm depending on the power employed. A major drawback is the small surface area of silicon that is heated.

JFE (Kawasaki Steel) has combined vacuum e-beam heating of a thin sheet of silicon, and e-beam heating with UDS.³⁵ That approach, effective in reducing the concentration of many impurities, including phosphorous, must be followed with a separate step to remove boron. The ingot from the UDS step is crushed and melted using a non-transferred arc plasma torch. An H₂-H₂O gas is used to volatilize boron. A conventional UDS step completes the process.

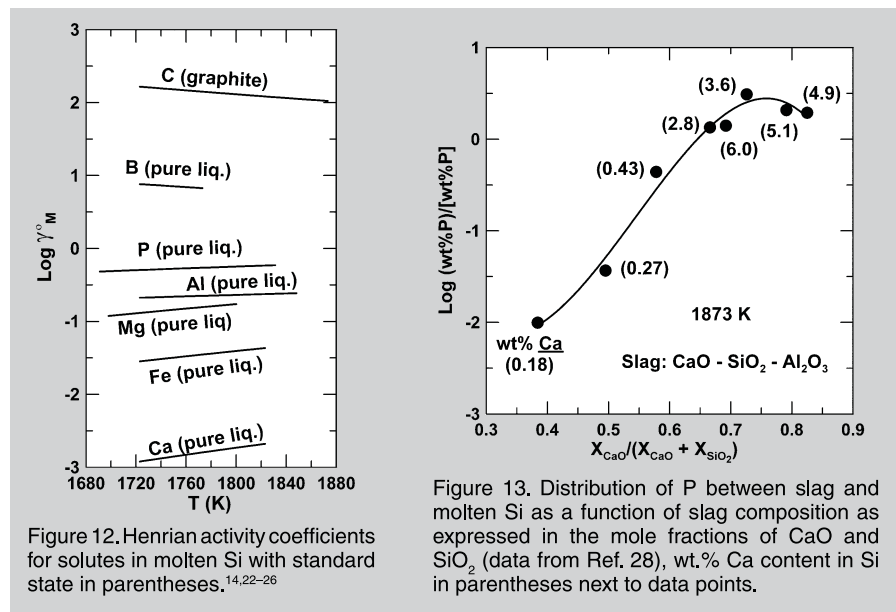


Figure 12. Henrian activity coefficients for solutes in molten Si with standard state in parentheses.^{14,22-26}

Figure 13. Distribution of P between slag and molten Si as a function of slag composition as expressed in the mole fractions of CaO and SiO₂ (data from Ref. 28), wt.% Ca content in Si in parentheses next to data points.

Slagging

Oxide slags with equilibrium mass distribution ratios of 2 and 3 for boron and phosphorous are severely limited in their ability to refine m-Si. Thus, fluxing agents free of boron and phosphorous are required to form a slag. Elkem Solar patented a concept for producing a low-phosphorous slag from inexpensive raw materials containing phosphorous by utilizing data in Figure 5.³⁶ Ferrosilicon with more than 65 wt.% iron provides for greater solubility of phosphorous in the melt versus molten silicon. Elkem Solar fused slag admixtures in the presence of ferrosilicon containing 80–90% iron to draw phosphorous from the slag into the ferrosilicon. The resulting slag is then used in the refining of m-Si. This approach allows for more freedom for utilizing a slag that has greater capacity for boron while still removing phosphorous.

The small distribution ratios obtained with an oxide slag for boron and phosphorous removal also require large mass of slag, far exceeding the mass of silicon refined. Elkem Solar³⁷ and Nippon Steel³⁸ in their patents approached this problem with counter current and semi-counter current processes that have the potential to reduce the mass of slag by an order of magnitude. In one patent³⁸ 10 to 100 batches of slag were allowed to equilibrate separately with silicon and then removed. Use of multiple reaction vessels in series has been proposed.³⁶

For a slag to act as an effective sink

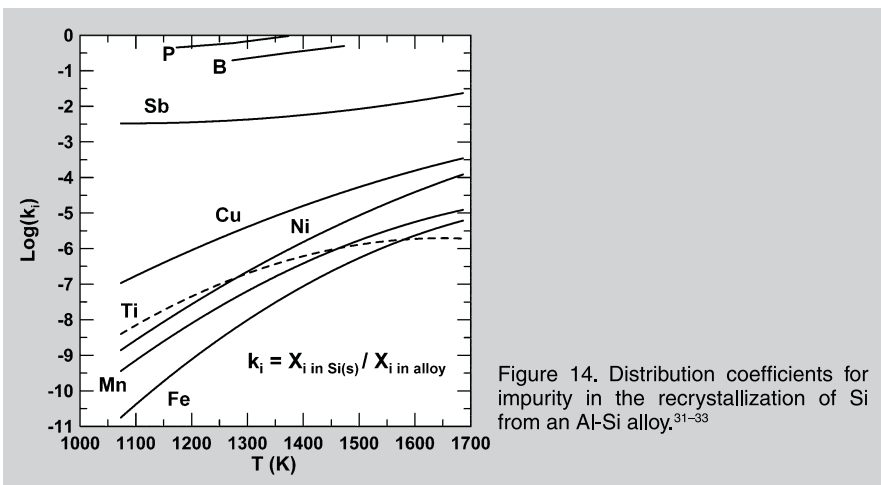


Figure 14. Distribution coefficients for impurity in the recrystallization of Si from an Al-Si alloy.^{31–33}

for both boron and phosphorous requires favorable thermodynamics for the exchange reactions involving transfer of impurity elements from silicon to slag, and a slag that has favorable bonding that reduces the activity coefficient of the constituents containing the impurity elements in slag. Oxide slag has little capacity for boron and phosphorous in refining silicon.

Of all the slag systems proposed, that containing Si_3N_4 has the greatest thermodynamic potential for removal of boron from silicon.^{39–41} The slagging operation involves an exchange reaction between the slag and molten silicon where Si_4N_4 in slag supplies nitrogen to remove boron from silicon through formation of BN that dissolves in slag. The advantage of this approach, beyond favorable thermodynamics, is that there are no counteracting effects as occurs in oxide slag with boron as observed in Figure 10. Lynch and Øye⁴¹ identified a system where activities of Si_3N_4 and Al_2O_3 in slag can have maximum values for transferring boron and phosphorous to slag as BN and AlP. Lynch and Øye also proposed how the composition of the slag can be adjusted to decrease the activity coefficients of boron and phosphorous, further improving the refining ability of slag.

Recrystallization of Silicon from Alloys

Recrystallization of silicon from an Al-Si alloy is only marginally effective in removing boron and phosphorous. This approach suffers from the same problem as oxide slag, namely the need to use alloying agents with a very low concentration of boron and phosphorous. With the Al-Si alloy the concen-

trations of boron and phosphorous will quickly rise above acceptable levels with silicon recrystallization. The alloy must either be cleansed of impurities or sold. The economic impact can be minimized by utilizing an alloying agent that has substantially smaller segregation coefficients for boron and phosphorous than with aluminum as solvent.

Removal of the molten alloy is a problem after recrystallization. Nichol has proposed⁴² decanting the alloy, using a high-temperature press to squeeze out trapped liquid. If necessary, the resulting slush can be remelted and recrystallization repeated. Reheating the silicon-rich slush will push the melting temperature toward the normal fusion temperature of silicon, thus much of the advantage of working with an alloy at lower temperatures is lost.

References

1. M.G. Mauk, P.E. Sims, and R.B. Hall, *AIP Conf. Proc.*, 404 (1) (1997), pp. 21–28.
2. B. Alpert, "Nightfall Comes to Solar Land," *Barrons On Line* (30 March 2009), <http://online.barrons.com/article/SB123820188149562545.html>.
3. RBC Capital Markets Report—RBC's Daily Snapshot, *Global Clean Energy Directions* (28 May 2009).
4. A. Feltrin and A. Freundlich, *Renewable Energy*, 33 (2) (2008), pp. 180–185.
5. W. Hoffmann, "Toward an Effective European Industrial Policy for Photovoltaics" (Paper presented at 20th EPIA AGM, Athens, Greece, 7–8 May 2004).
6. A. Schei, J.Kr. Tuset, and H. Tveit, *Production of High Silicon Alloys* (Trondheim, Norway: Tapir, 1998), p. 61.
7. E.H. Myrhaug and H. Tveit, "Material Balances of Trace Elements in the Ferrosilicon and Silicon Processes," *Electric Furnace Conference Proceedings – Vol. 58* (Warrendale, PA: AIST, 2000), pp. 591–604.
8. A. Schei, J.Kr. Tuset, and H. Tveit, in Ref. 6, p. 90.
9. D.C. Lynch, *Proceedings of the Silicon for the Chemical Industry VII*, ed. H.A. Øye, A. Holåa, and L. Nygaard (Trondheim, Norway: Dept. Mat. Tech. NTNU, 2004), pp. 17–31.
10. S. Ueda, K. Morita, and N. Sano, *Metall. & Mat. Trans. B*, 28B (6) (1997), pp. 1151–1155.
11. V. Dosaj, Dow Corning, private communication with author (May 2009).
12. G. Halvorsen, "Method for Production of Pure Sil-

- con," U.S. patent 4,539,194 (3 September 1985).
13. A. Schei, J.Kr. Tuset, and H. Tveit, in Ref. 6, pp. 285–291.
14. D.C. Lynch, *Proceedings of the Silicon for the Chemical Industry VI*, eds. H. A. Øye, H. Rong, L. Nygaard, G. Schüssler, and J. K. Tuset (Trondheim, Norway: Dept. Chem. NTNU, 2002), pp. 73–91.
15. H.C. Theuerer, *J. Metals*, 8 (1956), pp. 1316–1319.
16. N. Yuge et al., *Sol. Energy Mater. Sol. Cells*, 34 (1–4) (1994), pp. 243–250.
17. K. Suzuki and N. Sano, *10th Int. E.C. Photovoltaic Sol. Energy Conf. Proc.*, ed. L. Antonio (Dordrecht, Neth.: Kluwer, 1991), pp. 273–275.
18. H. Fujiwara et al., *JIM*, 60 (1) (1996), pp. 65–71.
19. D.C. Lynch and M. A. Lynch, in Ref. 9, pp. 307–318.
20. J.C.S. Pires et al., *J. Mat. Proc. Tech.*, 169 (1) (2005), pp. 21–25.
21. S. Tabuchi and N. Sano, *Metall. Trans. B*, 15B (6) (1984), pp. 351–356.
22. A.I. Zaitsev, N.E. Shelkova, and A.A. Kodentsov, *J. Phase Equilibria*, 21 (6) (2000), pp. 528–533.
23. T. Miki, K. Morita, and N. Sano, *Metall. & Mat. Trans. B*, 29B (5) (1998), pp. 1043–1049.
24. M. Tanahashi, T. Fujisawa, and C. Yamauchi, *Value-Addition Metallurgy*, ed. W.D. Cho and H.Y. Sohn (Warrendale, PA: TMS, 1998), pp. 103–109.
25. K. Yanaba et al., *Mat. Trans. JIM*, 38 (11) (1997), pp. 990–994.
26. T. Miki, K. Morita, and M. Yamawaki, *J. Mass Spectrom. Soc. Japan*, 47 (2) (1999), pp. 72–75.
27. C.H.P. Lupis, *Chemical Thermodynamics of Materials* (New York: Elsevier Sci., 1983), pp. 257–259.
28. H. Fujiwara et al., *Mat. Trans. JIM*, 37 (4) (1996), pp. 923–926.
29. W.G. Pfann, *Zone Melting*, 2nd ed. (New York: Wiley, 1966).
30. E.A. Good et al., *12th Workshop on Crystalline Silicon Solar Cell Materials and Processes: Extended Abstracts and Papers*, ed. B.L. Sopori (Golden, CO: NREL, 2002), pp. 236–239.
31. K. Morita and T. Yoshikwa, *Proceedings of the Silicon for the Chemical and Soar Industry IX*, ed. H.A. Øye et al. (Trondheim, Norway: Dept. Mat. Sci. and Engr. NTNU, 2008), pp. 51–59.
32. T. Yoshikwa and K. Morita, *Metall. & Mat. Trans. B*, 36B (4) (2005), pp. 731–736.
33. T. Yoshikwa and K. Morita, *Sci. & Tech. Adv. Mat.*, 4 (2003), pp. 531–537.
34. L. Nygaard, in Ref. 31, pp. 143–155.
35. N. Yuge et al., *Prog. Photovolt. Res. Appl.*, 9 (3) (2001), pp. 203–209.
36. E. Enebak et al., "A Calcium-Silicate Based Slag for Treatment of Molten Silicon," WIPO patent application 03/097528 A1 (27 November 2003).
37. A. Schei, "Method for Refining Silicon," EP patent 0 699 625 B1 (24 March 1999).
38. N. Ito et al., "Apparatus and Process for Producing High-Purity Silicon," EP patent application 1,958,923 A1 (20 November 2008).
39. J.V.D. Ayile, P. Ho, and J.M. Gee, *Silicon Purification Melting for Photovoltaic Applications- SAND 2000-0821* (Sandia National Laboratories, NM: DOE April 2000).
40. R. F. Clark et al., "Method and Application for Purifying Silicon," WIPO patent application 02/16265 (28 February 2002).
41. D. C. Lynch and H. A. Øye, "Silicon Refining Process," U.S. patent application 2007/0245854 A1 (25 October 2007).
42. S. Nichol, "Method for Purifying Silicon," WIPO patent application 2007/112592 A1 (11 October 2007).

David Lynch is Professor of both Mining Engineering and Materials Science and Engineering, and is also with the Lowell Institute for Mineral Resources at the University of Arizona, 12235 East James E. Rogers Way, Tucson, AZ 85721; (520) 626-6022; e-mail dclynch@email.arizona.edu.